$U(1)$ Extensions of SM and DM phenomenology

Sarif Khan

Harish-Chandra Research Institute, Allahabad

Talk at: **IISER Bhopal (WHEPP XV)**

Based on:
1608.04194, 1612.03067, 1704.00819, 1711.00553

In Collaboration With
Sandhya Choubey and Anirban Biswas

December 17, 2017

Talk Plan

- Motivation

Talk Plan

- Motivation
- $U(1)$ models

Talk Plan

- Motivation
- $U(1)$ models
- Results based on different $U(1)$ models

Talk Plan

- Motivation
- $U(1)$ models
- Results based on different $U(1)$ models
- Conclusion

Motivation

- Discovery of neutrino oscillation implies the existence of neutrino mass.

Motivation

- Discovery of neutrino oscillation implies the existence of neutrino mass.

- Almost 80% matter contents of the universe is unknown to us, namely Dark Matter (DM) [Many evidences which support the presence of DM].

Motivation

- Discovery of neutrino oscillation implies the existence of neutrino mass.
- Almost 80% matter contents of the universe is unknown to us, namely Dark Matter (DM) [Many evidences which support the presence of DM].
- Why there exist excess matter over antimatter in the universe.

Motivation

- Discovery of neutrino oscillation implies the existence of neutrino mass.
- Almost 80% matter contents of the universe is unknown to us, namely Dark Matter (DM) [Many evidences which support the presence of DM].
- Why there exist excess matter over antimatter in the universe.
- Disagreement between the theoretical and experimental value of muon $(g-2)$.

Standard Model (SM) $[SU(3)_c \times SU(2)_L \times U(1)_Y]$

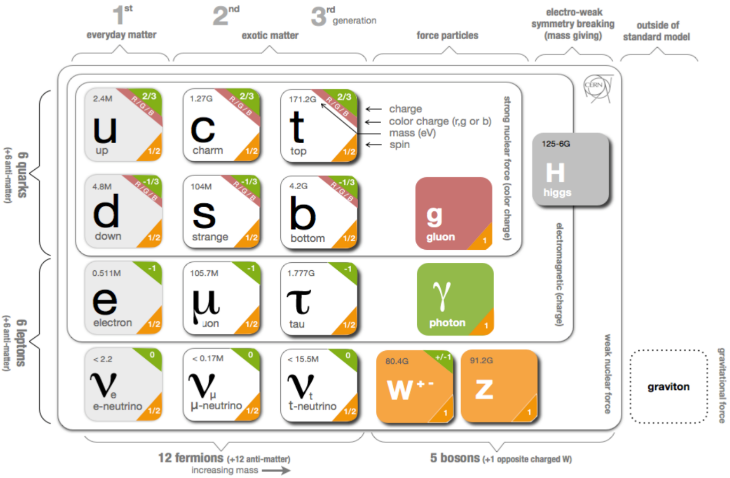

Figure: SM Particles list

$U(1)$ Models

- SM has accidental $U(1)$ global symmetry like baryon (B) and lepton (L) number conservation.

$U(1)$ Models

- SM has accidental $U(1)$ global symmetry like baryon (B) and lepton (L) number conservation.
- If we make these global transformation to lacal then it becomes anomolous.

$U(1)$ Models

- SM has accidental $U(1)$ global symmetry like baryon (B) and lepton (L) number conservation.
- If we make these global transformation to lacal then it becomes anomolous.
- Anomaly free situation can be achieved if we use the B and L combination instead of using them separately.

$U(1)$ Models

- SM has accidental $U(1)$ global symmetry like baryon (B) and lepton (L) number conservation.
- If we make these global transformation to lacal then it becomes anomolous.
- Anomaly free situation can be achieved if we use the B and L combination instead of using them separately.
- There are four anomaly free combinatoin which are B-L (flavor blind), $L_\mu - L_\tau$, $L_e - L_\mu$ and $L_e - L_\tau$.

- First we will discuss $U(1)_{L_\mu - L_\tau}$ extension.
  - Scalar DM including both WIMP (arXiv: 1608.04194) and FIMP (arXiv: 1612.03067).

- First we will discuss $U(1)_{L_\mu - L_\tau}$ extension.
  - Scalar DM including both WIMP (arXiv: 1608.04194) and FIMP (arXiv: 1612.03067).
  - Fermionic DM (arXiv: 1711.00553)

- Secondly we will discuss $U(1)_{B-L}$ extension.
  - Scalar DM, WIMP and FIMP (arXiv: 1704.00819).
  - Fermionic DM

Particles List and corresponding Charges [1]

Gauge Group	Baryon Fields			Lepton Fields			Scalar Fields		
	$Q_L^i = (u_L^i, d_L^i)^T$	u_R^i	d_R^i	$L_L^i = (\nu_L^i, e_L^i)^T$	e_R^i	N_R^i	ϕ_h	ϕ_H	ϕ_{DM}
$\mathrm{SU(2)_L}$	2	1	1	2	1	1	2	1	1
$\mathrm{U(1)_Y}$	1/6	2/3	−1/3	−1/2	−1	0	1/2	0	0

Figure: Particle contents and their corresponding charges under SM gauge group.

Gauge Group	Baryonic Fields	Lepton Fields			Scalar Fields		
	(Q_L^i, u_R^i, d_R^i)	(L_L^e, e_R, N_R^e)	$(L_L^\mu, \mu_R, N_R^\mu)$	$(L_L^\tau, \tau_R, N_R^\tau)$	ϕ_h	ϕ_H	ϕ_{DM}
$\mathrm{U(1)}_{L_\mu - L_\tau}$	0	0	1	−1	0	1	$n_{\mu\tau}$

Figure: Particle contents and their corresponding charges under $U(1)_{L_\mu - L_\tau}$.

[1] Based on JHEP 1609 (2016) 147, A. Biswas, SK, S. Choubey

Lagrangian of RH neutrino Sector:

$$\begin{aligned}\mathcal{L}_N &= \sum_{i=e,\,\mu,\,\tau} \frac{i}{2}\bar{N}_i\gamma^\mu D_\mu N_i - \frac{1}{2}\,M_{ee}\,\bar{N}^c_e N_e - \frac{1}{2}\,M_{\mu\tau}\,(\bar{N}^c_\mu N_\tau + \bar{N}^c_\tau N_\mu) \\ &\quad -\frac{1}{2}\,h_{e\mu}(\bar{N}^c_e N_\mu + \bar{N}^c_\mu N_e)\phi^\dagger_H - \frac{1}{2}\,h_{e\tau}(\bar{N}^c_e N_\tau + \bar{N}^c_\tau N_e)\phi_H \\ &\quad - \sum_{i=e,\,\mu,\,\tau} y_i \bar{L}_i\tilde{\phi}_h N_i + h.c. \end{aligned} \tag{1}$$

where $\tilde{\phi}_h = i\,\sigma_2\phi^*_h$.

Lagrangian of DM Sector:

$$\begin{aligned}\mathcal{L}_{DM} &= (D^\mu\phi_{DM})^\dagger(D_\mu\phi_{DM}) - \mu^2_{DM}\phi^\dagger_{DM}\phi_{DM} - \lambda_{DM}(\phi^\dagger_{DM}\phi_{DM})^2 \\ &\quad -\lambda_{Dh}(\phi^\dagger_{DM}\phi_{DM})(\phi^\dagger_h\phi_h) - \lambda_{DH}(\phi^\dagger_{DM}\phi_{DM})(\phi^\dagger_H\phi_H)\,. \end{aligned} \tag{2}$$

and

$$V(\phi_h,\phi_H) = \mu^2_H\phi^\dagger_H\phi_H + \lambda_H(\phi^\dagger_H\phi_H)^2 + \lambda_{hH}(\phi^\dagger_h\phi_h)(\phi^\dagger_H\phi_H)\,. \tag{3}$$

Complete Lagrangian,

$$\mathcal{L} = \mathcal{L}_{SM} + \mathcal{L}_N + \mathcal{L}_{DM} + V(\phi_h,\phi_H). \tag{4}$$

Results

Muon $(g-2)$

- Magnetic Moment: It is defined in the following way,

$$\vec{M} = g_\mu \frac{e}{2\, m_\mu} \vec{S}, \tag{5}$$

In general $g_\mu = 2$, and if we consider all the effects of loop diagrams then it differs from the experimentally observed value, which is,

$$\Delta a_\mu = a_\mu^{\rm exp} - a_\mu^{\rm th} = (29.0 \pm 9.0) \times 10^{-10}\,. \tag{6}$$

Results

Muon $(g-2)$

- Magnetic Moment: It is defined in the following way,

$$\vec{M} = g_\mu \frac{e}{2\, m_\mu} \vec{S}, \tag{5}$$

In general $g_\mu = 2$, and if we consider all the effects of loop diagrams then it differs from the experimentally observed value, which is,

$$\Delta a_\mu = a_\mu^{\rm exp} - a_\mu^{\rm th} = (29.0 \pm 9.0) \times 10^{-10}\,. \tag{6}$$

- In the present model due to gauged extention we have extra gauge boson, $Z_{\mu\tau}$.

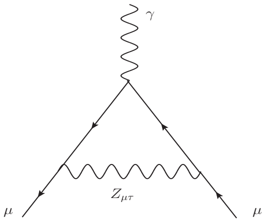

Figure: One loop Feynman diagram contributing to muon $(g-2)$, mediated by the extra gauge boson $Z_{\mu\tau}$.

- Contribution from the above diagram is,

$$\Delta a_\mu(Z_{\mu\tau}) = \frac{g_{\mu\tau}^2}{8\pi^2}\int_0^1 dx \frac{2x(1-x)^2}{(1-x)^2 + rx}\,, \tag{7}$$

where, $r = (M_{Z_{\mu\tau}}/m_\mu)^2$.

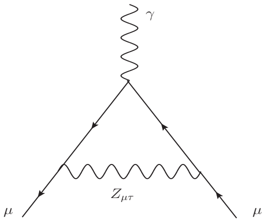

Figure: One loop Feynman diagram contributing to muon $(g-2)$, mediated by the extra gauge boson $Z_{\mu\tau}$.

- Contribution from the above diagram is,

$$\Delta a_\mu(Z_{\mu\tau}) = \frac{g_{\mu\tau}^2}{8\pi^2}\int_0^1 dx \frac{2x(1-x)^2}{(1-x)^2+rx}\,, \quad (7)$$

where, $r = (M_{Z_{\mu\tau}}/m_\mu)^2$.

- For the present choosen values, $M_{Z_{\mu\tau}} = 100$ MeV and $g_{\mu\tau} = 9\times10^{-4}$ the value of $\Delta a_\mu = 22.6\times10^{-10}$, lies within the above mentioned range.

Neutrino Mixing angles

We have used the following constraints on neutrino oscillation parameters ,

- Cosmological upper bound on the sum of all three light neutrinos, $\sum_i m_i < 0.23$ eV at 2σ C.L. [2],

[2]Planck Coll. 1502.01589
[3]Capozzi et, al.,1601.07777
[4]Capozzi et al,1601.07777

Neutrino Mixing angles

We have used the following constraints on neutrino oscillation parameters ,

- Cosmological upper bound on the sum of all three light neutrinos, $\sum_i m_i < 0.23$ eV at 2σ C.L. [2],
- Mass squared differences $6.93 < \frac{\Delta m^2_{21}}{10^{-5}}\,\text{eV}^2 < 7.97$ and $2.37 < \frac{\Delta m^2_{31}}{10^{-3}}\,\text{eV}^2 < 2.63$ in 3σ range [3],

[2] Planck Coll. 1502.01589

[3] Capozzi et, al.,1601.07777

[4] Capozzi et al,1601.07777

Neutrino Mixing angles

We have used the following constraints on neutrino oscillation parameters ,

- Cosmological upper bound on the sum of all three light neutrinos, $\sum_i m_i < 0.23$ eV at 2σ C.L. [2],
- Mass squared differences $6.93 < \frac{\Delta m^2_{21}}{10^{-5}}\,\mathrm{eV}^2 < 7.97$ and $2.37 < \frac{\Delta m^2_{31}}{10^{-3}}\,\mathrm{eV}^2 < 2.63$ in 3σ range [3],
- All three mixing angles $30^\circ < \theta_{12} < 36.51^\circ$, $37.99^\circ < \theta_{23} < 51.71^\circ$ and $7.82^\circ < \theta_{13} < 9.02^\circ$ also in 3σ range [4].

[2] Planck Coll. 1502.01589

[3] Capozzi et, al.,1601.07777

[4] Capozzi et al,1601.07777

- Majorana mass matrix $\mathcal{M}_R$ has the following form and its (2,2) and (3,3) elements are zero due to $\mathrm{U}(1)_{L_\mu - L_\tau}$ symmetry

$$\mathcal{M}_R = \begin{pmatrix} M_{ee} & \frac{v_{\mu\tau}}{\sqrt{2}} h_{e\mu} & \frac{v_{\mu\tau}}{\sqrt{2}} h_{e\tau} \\ \frac{v_{\mu\tau}}{\sqrt{2}} h_{e\mu} & 0 & M_{\mu\tau}\, e^{i\xi} \\ \frac{v_{\mu\tau}}{\sqrt{2}} h_{e\tau} & M_{\mu\tau}\, e^{i\xi} & 0 \end{pmatrix}, \quad (8)$$

- Majorana mass matrix $\mathcal{M}_R$ has the following form and its (2,2) and (3,3) elements are zero due to $\mathrm{U}(1)_{L_\mu - L_\tau}$ symmetry

$$\mathcal{M}_R = \begin{pmatrix} M_{ee} & \frac{v_{\mu\tau}}{\sqrt{2}} h_{e\mu} & \frac{v_{\mu\tau}}{\sqrt{2}} h_{e\tau} \\ \frac{v_{\mu\tau}}{\sqrt{2}} h_{e\mu} & 0 & M_{\mu\tau}\, e^{i\xi} \\ \frac{v_{\mu\tau}}{\sqrt{2}} h_{e\tau} & M_{\mu\tau}\, e^{i\xi} & 0 \end{pmatrix}, \quad (8)$$

- Dirac mass matrix is diagonal due to $\mathrm{U}(1)_{L_\mu - L_\tau}$ symmetry.

- Neutrino masses will be generated by the Type I seesaw mechanism by the following relation,

$$m_\nu \simeq -M_D\, M_R^{-1} M_D^T\,, \quad (9)$$
$$m_N \simeq M_R\,. \quad (10)$$

- Full expression of the light netrino mass matrix is,

$$m_\nu = \frac{1}{2\,p}\begin{pmatrix} 2\,f_e^2 M_{\mu\tau}^2 e^{i\xi} & -\sqrt{2}\,f_e f_\mu\, h_{e\tau} v_{\mu\tau} & -\sqrt{2}\,f_e f_\tau\, h_{e\mu} v_{\mu\tau} \\ -\sqrt{2}\,f_e f_\mu\, h_{e\tau} v_{\mu\tau} & \dfrac{f_\mu^2\, h_{e\tau}^2\, v_{\mu\tau}^2\, e^{-i\xi}}{M_{\mu\tau}} & \dfrac{f_\mu\, f_\tau}{M_{\mu\tau}}(M_{ee}\, M_{\mu\tau} - p\, e^{-i\xi}) \\ -\sqrt{2}\,f_e f_\tau\, h_{e\mu} v_{\mu\tau} & \dfrac{f_\mu\, f_\tau}{M_{\mu\tau}}(M_{ee}\, M_{\mu\tau} - p\, e^{-i\xi}) & \dfrac{f_\tau^2\, h_{e\mu}^2\, v_{\mu\tau}^2\, e^{-i\xi}}{M_{\mu\tau}} \end{pmatrix}$$

where $p = h_{e\mu}\, h_{e\tau}\, v_{\mu\tau}^2 - M_{ee}\, M_{\mu\tau}\, e^{i\xi}$.

- We used Armadillo (C++ linear algebra library) to diagonalize the above mentioned neutrino mass matrix.

- We used Armadillo (C++ linear algebra library) to diagonalize the above mentioned neutrino mass matrix.
- At the time of diagonalisation we have varied the parameters in the following range,

$$\begin{array}{ccccc} 0 & \leq & \xi\,[\text{rad}] & \leq & 2\pi\ , \\ 1 & \leq & M_{ee},\ M_{\mu\tau}\,[\text{GeV}] & \leq & 10^4\ , \\ 1 & \leq & V_{e\mu},\ \ V_{e\tau}\ \ [\text{GeV}] & \leq & 280\ , \\ 0.1 & \leq & \dfrac{(f_e,\ f_\mu,\ f_\tau)}{10^{-4}}\,[\text{GeV}] & \leq & 10\ . \end{array} \tag{11}$$

- We used Armadillo (C++ linear algebra library) to diagonalize the above mentioned neutrino mass matrix.
- At the time of diagonalisation we have varied the parameters in the following range,

$$\begin{array}{ccccc} 0 & \leq & \xi\,[\text{rad}] & \leq & 2\pi\ , \\ 1 & \leq & M_{ee},\, M_{\mu\tau}\,[\text{GeV}] & \leq & 10^4\ , \\ 1 & \leq & V_{e\mu},\ \ V_{e\tau}\ \ [\text{GeV}] & \leq & 280\ , \\ 0.1 & \leq & \dfrac{(f_e,\ f_\mu,\ f_\tau)}{10^{-4}}\,[\text{GeV}] & \leq & 10\ . \end{array} \qquad (11)$$

- There are correlations among the parameters to satisfy the neutrino oscillation parametrs.

Scatter Plot

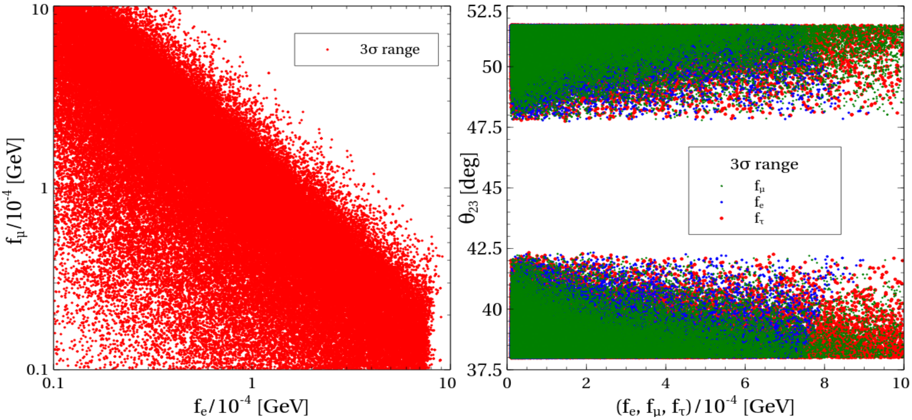

Figure: Scatter Plot: Left Panel - f_e vs f_μ, Right Panel - θ_{23} vs f_e, f_μ and f_τ

Scatter Plot

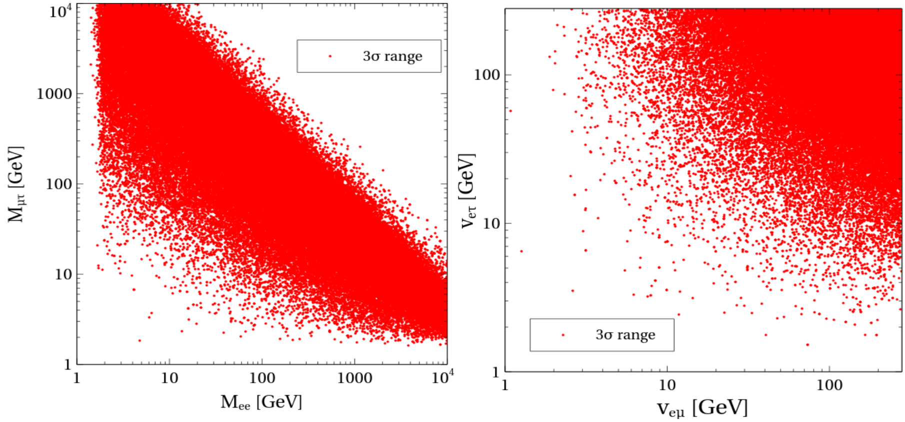

Figure: Scatter Plot: Left Panel - $M_{\mu\tau}$ vs M_{ee}, Right Panel - $V_{e\tau}$ vs $V_{e\mu}$.

Dark Matter (WIMP)

- In studying the DM we have implemented the model Lagrangian in LanHEP Package.

Dark Matter (WIMP)

- In studying the DM we have implemented the model Lagrangian in LanHEP Package.
- From LanHEP we have generated CalcHEP file to study DM phenomenology by using micrOMEGAs Package.

Constraints

- Planck and WMAP have measured DM relic density very precisely, which is $\Omega h^2 = 0.1199 \pm 0.0027$.

[5] Calore et. al. arXiv:1411.4647

Constraints

- Planck and WMAP have measured DM relic density very precisely, which is $\Omega h^2 = 0.1199 \pm 0.0027$.
- We have used the SI DD cross section bound from diff. ongoing earth based expt.

[5] Calore et. al. arXiv:1411.4647

Constraints

- Planck and WMAP have measured DM relic density very precisely, which is $\Omega h^2 = 0.1199 \pm 0.0027$.
- We have used the SI DD cross section bound from diff. ongoing earth based expt.
- To explain Fermi-LAT GC γ-ray excess, there is a bound on DM mass ($48.7^{+6.4}_{-5.2}$ GeV) and annihilation cross section to $b\bar{b}$ ($\langle \sigma \mathrm{v}_{b\bar{b}} \rangle = 1.75^{+0.28}_{-0.26} \times 10^{-26}$ cm^3/s) [5]

[5] Calore et. al. arXiv:1411.4647

Constraints

- Planck and WMAP have measured DM relic density very precisely, which is $\Omega h^2 = 0.1199 \pm 0.0027$.
- We have used the SI DD cross section bound from diff. ongoing earth based expt.
- To explain Fermi-LAT GC γ-ray excess, there is a bound on DM mass ($48.7^{+6.4}_{-5.2}$ GeV) and annihilation cross section to $b\bar{b}$ ($\langle \sigma \mathrm{v}_{b\bar{b}} \rangle = 1.75^{+0.28}_{-0.26} \times 10^{-26}$ cm^3/s) [5]
- We have considered bound on BR of Higgs decay to invisible particles which is less than 20%.

[5] Calore et. al. arXiv:1411.4647

Constraints

- Planck and WMAP have measured DM relic density very precisely, which is $\Omega h^2 = 0.1199 \pm 0.0027$.
- We have used the SI DD cross section bound from diff. ongoing earth based expt.
- To explain Fermi-LAT GC γ-ray excess, there is a bound on DM mass ($48.7^{+6.4}_{-5.2}$ GeV) and annihilation cross section to $b\bar{b}$ ($\langle \sigma \mathrm{v}_{b\bar{b}} \rangle = 1.75^{+0.28}_{-0.26} \times 10^{-26}$ cm^3/s) [5]
- We have considered bound on BR of Higgs decay to invisible particles which is less than 20%.
- Vacuum stability of the Higgs potential and perturbative limit on the coupling constants.

[5] Calore et. al. arXiv:1411.4647

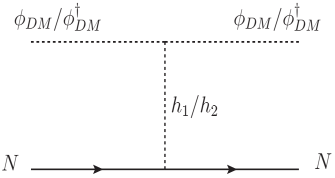

Figure: DM Direct Detection scattering diagram with the nuclei.

The expression of spin independent scattering cross section of DM with nucleon (N) is given by

$$\sigma_{\rm SI} = \frac{\mu^2}{4\pi}\left[\frac{M_N\, f_N\, \cos\alpha}{M_{DM}\, v}\left(\frac{\tan\alpha\, g_{\phi_{DM}\phi^{\dagger}_{DM}h_2}}{M^2_{h_2}} - \frac{g_{\phi_{DM}\phi^{\dagger}_{DM}h_1}}{M^2_{h_1}}\right)\right]^2, \tag{12}$$

where μ is the reduced mass between DM and nucleon.

Results (WIMP Part)

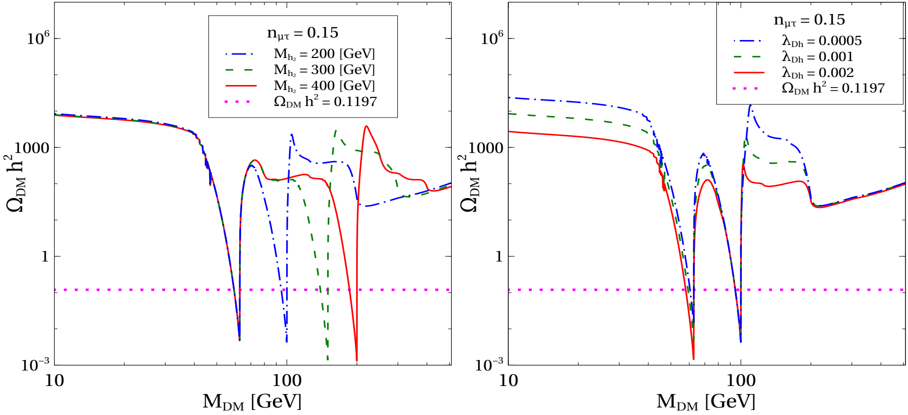

Results (WIMP Part)

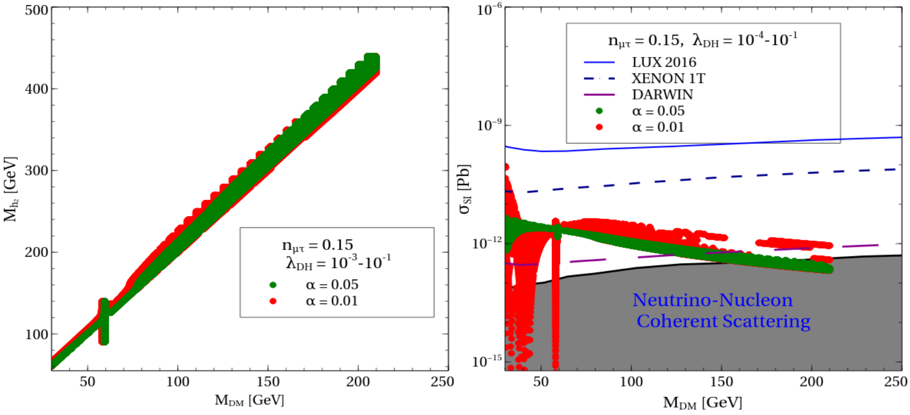

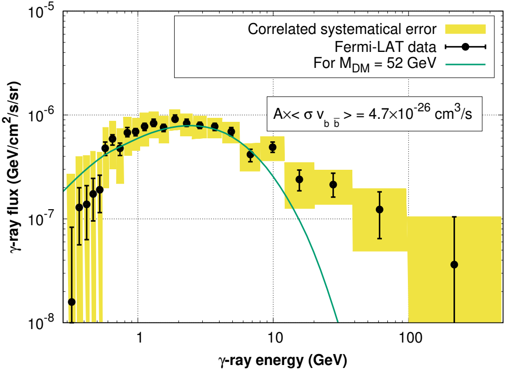

Figure: Gamma-ray flux obtained from the pair annihilation of ϕ_{DM} and $\phi^\dagger_{DM}$ at the Galactic Centre for $M_{DM} = 52$ GeV, $\langle \sigma \mathrm{v}_{b\bar{b}} \rangle = 3.856 \times 10^{-26}\,\mathrm{cm}^3/\mathrm{s}$ and $\mathcal{A} = 1.219$

FIMP DM in $U(1)_{L_\mu - L_\tau}$

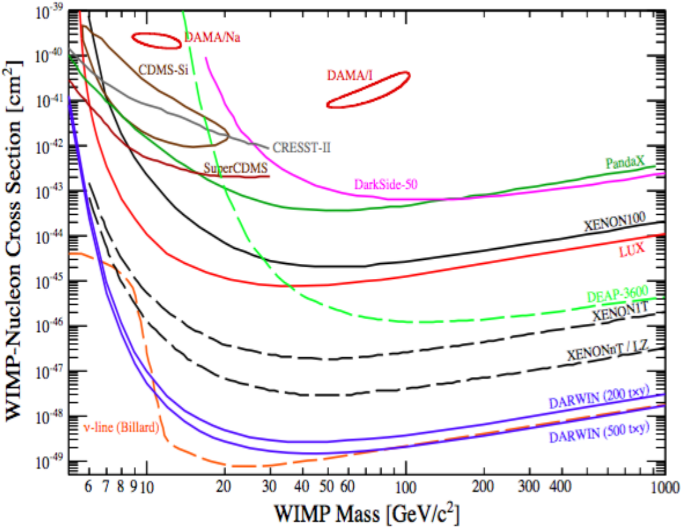

Figure: DD bound from diff. ongoing (proposed) experiments.

- No real signals have been observed in the DD experiments.

- No real signals have been observed in the DD experiments.
- Very soon DD limit on the SI cross section is going to touch the neutrino floar.

- No real signals have been observed in the DD experiments.
- Very soon DD limit on the SI cross section is going to touch the neutrino floar.
- Need to introduce new techniques to distinguish the DM signals from the neutrino signal.

- No real signals have been observed in the DD experiments.
- Very soon DD limit on the SI cross section is going to touch the neutrino floar.
- Need to introduce new techniques to distinguish the DM signals from the neutrino signal.
- Another way to tackle this problem is to propose a different way of DM production in the early universe rather than the well known freeze out mechanism.

- No real signals have been observed in the DD experiments.
- Very soon DD limit on the SI cross section is going to touch the neutrino floar.
- Need to introduce new techniques to distinguish the DM signals from the neutrino signal.
- Another way to tackle this problem is to propose a different way of DM production in the early universe rather than the well known freeze out mechanism.
- Many physicist have proposed a new way of DM production in the early universe, one of them is the freeze in mechanism.

Few words about Freeze-In mechanism

- In this mechanism in the early universe DM relic density is assumed to be zero.

Few words about Freeze-In mechanism

- In this mechanism in the early universe DM relic density is assumed to be zero.
- DM produced from the decay or annihilation of other particles.

Few words about Freeze-In mechanism

- In this mechanism in the early universe DM relic density is assumed to be zero.
- DM produced from the decay or annihilation of other particles.
- The coupling strength of DM with the cosmic soup is very feeble which is $\mathcal{O}(10^{-10})$.

Few words about Freeze-In mechanism

- In this mechanism in the early universe DM relic density is assumed to be zero.
- DM produced from the decay or annihilation of other particles.
- The coupling strength of DM with the cosmic soup is very feeble which is $\mathcal{O}(10^{-10})$.
- Since the coupling strength is very feeble, DM never attains thermal equilibrium with the cosmic soup.

Few words about Freeze-In mechanism

- In this mechanism in the early universe DM relic density is assumed to be zero.
- DM produced from the decay or annihilation of other particles.
- The coupling strength of DM with the cosmic soup is very feeble which is $\mathcal{O}(10^{-10})$.
- Since the coupling strength is very feeble, DM never attains thermal equilibrium with the cosmic soup.
- Due to very feeble coupling it hardly interacts with the rest or in other words it is very feebly interacting, hence the name FIMP.

Few words about Freeze-In mechanism

- In this mechanism in the early universe DM relic density is assumed to be zero.
- DM produced from the decay or annihilation of other particles.
- The coupling strength of DM with the cosmic soup is very feeble which is $\mathcal{O}(10^{-10})$.
- Since the coupling strength is very feeble, DM never attains thermal equilibrium with the cosmic soup.
- Due to very feeble coupling it hardly interacts with the rest or in other words it is very feebly interacting, hence the name FIMP.
- Since the DM FIMP type, no as such detection technique like WIMP.

Procedure to calculate DM Relic density

- Need to find all the production channels by which DM can produce.

Procedure to calculate DM Relic density

- Need to find all the production channels by which DM can produce.
- To determine the co-moving number density (Y) we will solve the relevant Boltzmann equation.

Procedure to calculate DM Relic density

- Need to find all the production channels by which DM can produce.
- To determine the co-moving number density (Y) we will solve the relevant Boltzmann equation.
- In solving the BE, we will take initial condition, $Y = 0$ for $T = T_{ini}$.

Procedure to calculate DM Relic density

- Need to find all the production channels by which DM can produce.
- To determine the co-moving number density (Y) we will solve the relevant Boltzmann equation.
- In solving the BE, we will take initial condition, $Y = 0$ for $T = T_{ini}$.
- Once we find the co-moving number density, we can easily determine the DM relic density using following relation

$$\Omega_{\phi_{DM}} h^2 = 2.755 \times 10^8 \left(\frac{M_{\phi_{DM}}}{\mathrm{GeV}}\right) Y_{\phi_{DM}}(T_0) \,.$$

Results

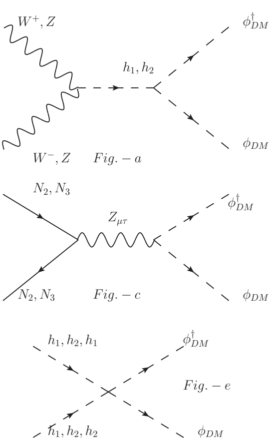

Figure: Relevant Feynman Diagrams

$$
\begin{aligned}
\frac{dY_{\phi_{DM}}}{dz} &= \frac{2M_{pl}}{1.66 M_{h_2}^2} \frac{z\sqrt{g_\star(z)}}{g_s(z)} \left[\sum_{i=1,\,2} \langle \Gamma_{h_i \to \phi_{DM}^\dagger \phi_{DM}} \rangle (Y_i^{eq} - Y_{\phi_{DM}}) \right] \\
&+ \frac{4\pi^2}{45} \frac{M_{pl} M_{h_2}}{1.66} \frac{\sqrt{g_\star(z)}}{z^2} \\
&\times \left[\sum_{p=W,Z,h_1,h_2,f} \langle \sigma \mathrm{v}_{p\bar{p} \to \phi_{DM}^\dagger \phi_{DM}} \rangle (Y_p^{eq\;2} - Y_{\phi_{DM}}^2) \right. \\
&+ \sum_{i=1,j=2,3} \langle \sigma \mathrm{v}_{N_i N_j \to \phi_{DM}^\dagger \phi_{DM}} \rangle (Y_{N_i}^{eq} Y_{N_j}^{eq} - Y_{\phi_{DM}}^2) \\
&\left. + \langle \sigma \mathrm{v}_{h_1 h_2 \to \phi_{DM}^\dagger \phi_{DM}} \rangle (Y_{h_1}^{eq} Y_{h_2}^{eq} - Y_{\phi_{DM}}^2) \right] .
\end{aligned}
$$

Expression of $\langle \sigma v_{A\,B \to \phi^\dagger_{DM} \phi_{DM}} \rangle$ and $\langle \Gamma_{h_i \to \phi^\dagger_{DM} \phi_{DM}} \rangle$ are given by

$$
\begin{aligned}
f_1 &= \sqrt{s^2 + (M_A^2 - M_B^2)^2 - 2\,s\,(M_A^2 + M_B^2)}\,, \\
f_2 &= \sqrt{s - (M_A - M_B)^2}\ \sqrt{s - (M_A + M_B)^2}\ , \\
\langle \sigma v_{A\,B \to \phi^\dagger_{DM} \phi_{DM}} \rangle &= \frac{1}{8\,M_A^2\,M_B^2\,T\,K_2\left(\frac{M_A}{T}\right)\ K_2\left(\frac{M_B}{T}\right)} \times \\
& \int_{(M_A+M_B)^2}^{\infty} \frac{\sigma_{A\,B \to \phi^\dagger_{DM} \phi_{DM}}}{\sqrt{s}}\ f_1\ f_2\ K_1\left(\frac{\sqrt{s}}{T}\right)\ \mathrm{d}s\,, \\
\langle \Gamma_{h_i \to \phi^\dagger_{DM} \phi_{DM}} \rangle &= \frac{K_1(z)}{K_2(z)}\ \Gamma_{i \to \phi^\dagger_{DM} \phi_{DM}}\,.
\end{aligned}
$$

Relavant Couplings of DM ϕ_{DM}

Vertex $a\,b\,c$	Vertex Factor g_{abc}
$\phi_{DM}\,\phi_{DM}^{\dagger}\,h_1$	$-(\lambda_{Dh} v \cos\alpha + \lambda_{DH} v_{\mu\tau} \sin\alpha)$
$\phi_{DM}\,\phi_{DM}^{\dagger}\,h_2$	$(\lambda_{Dh} v \sin\alpha - \lambda_{DH} v_{\mu\tau} \cos\alpha)$
$\phi_{DM}\,\phi_{DM}^{\dagger}\,Z_{\mu\tau}^{\rho}$	$n_{\mu\tau} g_{\mu\tau} (p_2 - p_1)^{\rho}$
$\bar{N}_i\,N_i\,Z_{\mu\tau}^{\rho}$	$\frac{g_{\mu\tau}}{2}\gamma^{\rho}\gamma^{5}$

Table: Relevant couplings required to compute Feynman diagrams

Results

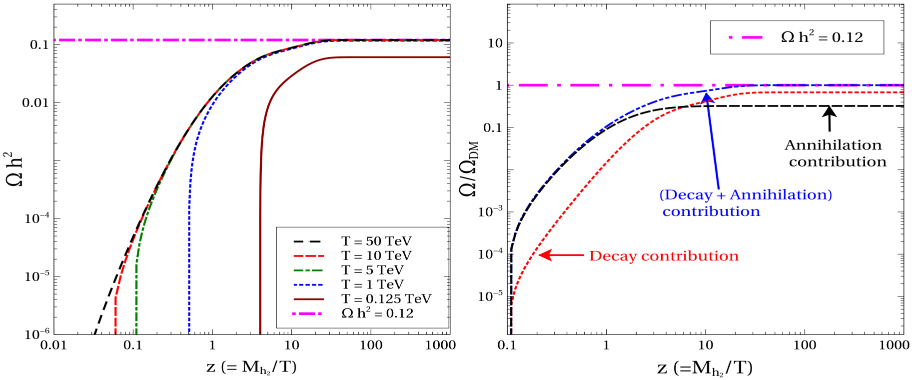
0.1
0.01
10^{-4}
10^{-5}
10^{-6}
Ωh^2
0.01
0.1
1
10
100
1000
z (= M_{h_2}/T)
T = 50 TeV
T = 10 TeV
T = 5 TeV
T = 1 TeV
T = 0.125 TeV
$\Omega h^2 = 0.12$
10
1
0.1
10^{-3}
10^{-4}
10^{-5}
Ω/Ω_{DM}
0.1
1
10
100
1000
z (=M_{h_2}/T)
$\Omega h^2 = 0.12$
Annihilation contribution
(Decay + Annihilation) contribution
Decay contribution

Results (Scatter Plots)

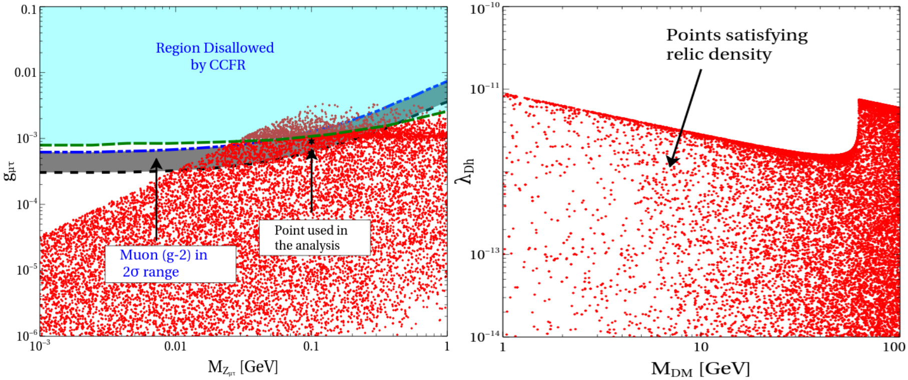

Results (Scatter Plots)

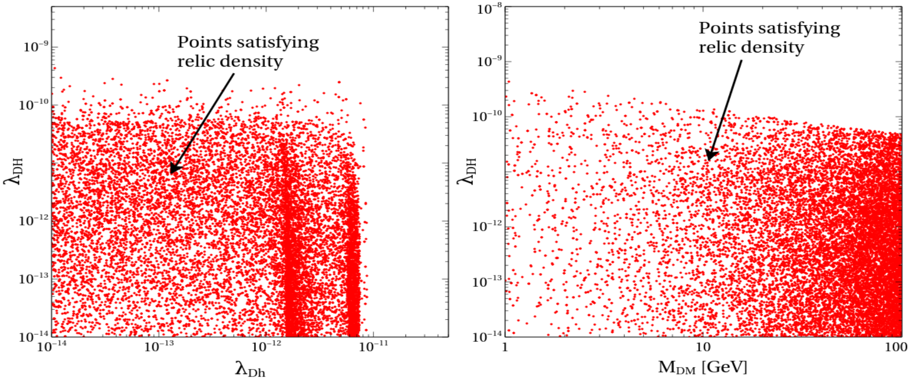

Fermionc FIMP DM in $U(1)_{L_\mu - L_\tau}$ model
Based on arXiv: 1711.00553[6]

Gauge Group	Baryon Fields			Lepton Fields			Scalar Fields		
	$Q_L^i = (u_L^i, d_L^i)^T$	u_R^i	d_R^i	$L_L^i = (\nu_L^i, e_L^i)^T$	e_R^i	N_R^i	ϕ_h	ϕ_H	η
$\mathrm{SU(2)_L}$	2	1	1	2	1	1	2	1	2
$\mathrm{U(1)_Y}$	1/6	2/3	−1/3	−1/2	−1	0	1/2	0	1/2
$\mathbb{Z}_2$	+	+	+	+	+	−	+	+	−

Table: Particle contents and their corresponding charges under SM gauge group and discrete group $\mathbb{Z}_2$.

Gauge Group	Baryonic Fields	Lepton Fields			Scalar Fields		
	(Q_L^i, u_R^i, d_R^i)	(L_L^e, e_R, N_R^e)	$(L_L^\mu, \mu_R, N_R^\mu)$	$(L_L^\tau, \tau_R, N_R^\tau)$	ϕ_h	ϕ_H	η
$\mathrm{U(1)}_{L_\mu - L_\tau}$	0	0	1	−1	0	1	0

Table: Particle contents and their corresponding charges under $\mathrm{U(1)}_{L_\mu - L_\tau}$.

[6] In detail by A. Biswas

Lagrangian

$$
\begin{aligned}
\mathcal{L} &= \mathcal{L}_{SM} + \mathcal{L}_N + (D_\mu \phi_H)^\dagger (D^\mu \phi_H) + (D_\mu \eta)^\dagger (D^\mu \eta) \\
&\quad -\frac{1}{4} F_{\mu\tau\,\rho\sigma} F_{\mu\tau}{}^{\rho\sigma} - V(\phi_h, \phi_H, \eta)\,, \qquad (13)
\end{aligned}
$$

where $\mathcal{L}_N$ takes the following form,

$$
\begin{aligned}
\mathcal{L}_N &= \sum_{i=e,\,\mu,\,\tau} \frac{i}{2} \bar{N}_i \gamma^\mu D_\mu N_i - \frac{1}{2}\, M_{ee}\, \bar{N}_e^c N_e - \frac{1}{2}\, M_{\mu\tau}\, (\bar{N}_\mu^c N_\tau + \bar{N}_\tau^c N_\mu) \\
&\quad -\frac{1}{2}\, h_{e\mu} (\bar{N}_e^c N_\mu + \bar{N}_\mu^c N_e) \phi_H^\dagger - \frac{1}{2}\, h_{e\tau} (\bar{N}_e^c N_\tau + \bar{N}_\tau^c N_e) \phi_H \\
&\quad - \sum_{\alpha=e,\,\mu,\,\tau} h_\alpha \bar{L_\alpha} \tilde{\eta} N_\alpha + h.c.\,, \qquad (14)
\end{aligned}
$$

3.55 keV line

RH neutrino mass matrix takes the following form after gauged $L_\mu - L_\tau$ symmetry breaking,

$$\mathcal{M}_R = \begin{pmatrix} M_{ee} & \frac{v_{\mu\tau}}{\sqrt{2}} h_{e\mu} & \frac{v_{\mu\tau}}{\sqrt{2}} h_{e\tau} \\ \frac{v_{\mu\tau}}{\sqrt{2}} h_{e\mu} & 0 & M_{\mu\tau}\, e^{i\xi} \\ \frac{v_{\mu\tau}}{\sqrt{2}} h_{e\tau} & M_{\mu\tau}\, e^{i\xi} & 0 \end{pmatrix}, \tag{15}$$

We can naturally generate mass spliting of 3.5 keV between the two RH neutrinos for small values of $h_{e\mu(\tau)}$ which is,

$$\Delta M_{23} = \frac{(h_{e\mu} + h_{e\tau})^2 v_{\mu\tau}^2}{2M_{ee}}. \tag{16}$$

From the decay of $N_2 \to N_3\gamma$, one can explain 3.5 keV line from this model.

Radiative neutrino mass

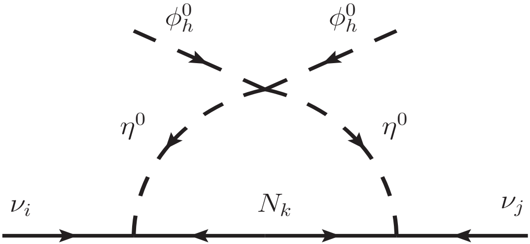

Figure: Radiative neutrino mass generation by one loop.

giving the following mass matrix for the light neutrinos by using E. Ma model

$$M^{\nu}_{ij} = \sum_k \frac{y_{ik}\, y_{jk}\, M_k}{16\,\pi^2} \left[\frac{M^2_{\eta^0_R}}{M^2_{\eta^0_R} - M^2_k} \ln \frac{M^2_{\eta^0_R}}{M^2_k} - \frac{M^2_{\eta^0_I}}{M^2_{\eta^0_I} - M^2_k} \ln \frac{M^2_{\eta^0_I}}{M^2_k} \right] , \quad (17)$$

where $y_{ik} = h_j U_{jk}$.

FIMP fermionic DM

RH neutrinos are feebly interacting hence, $g_{\mu\tau}$ are small. Therefore, we need to determine the $Z_{\mu\tau}$ distribution function by solving the following BE,

$$\hat{L} f_{Z_{\mu\tau}} = \sum_{i=1,2} \mathcal{C}^{h_i \rightarrow Z_{\mu\tau} Z_{\mu\tau}} + \mathcal{C}^{Z_{\mu\tau} \rightarrow \, all}\,, \tag{18}$$

where

$$\hat{L} = r\, H \left(1 + \frac{T g_s'}{3 g_s}\right)^{-1} \frac{\partial}{\partial\, r} \tag{19}$$

Now comoving number density of RH neutrinos (DM) can be determined by the following BE,

$$\begin{aligned} \frac{dY_{N_j}}{dr} &= \frac{V_{ij}\, M_{pl}\, r\, \sqrt{g_\star(r)}}{1.66\, M_{sc}^2\, g_s(r)} \left[\sum_{k=1,2} \sum_{i=1,2,3} \langle \Gamma_{h_k \rightarrow N_j\, N_i} \rangle (Y_{h_k} - Y_{N_j} Y_{N_i})\right] \\ &+ \frac{V_{ij}\, M_{pl}\, r\, \sqrt{g_\star(r)}}{1.66\, M_{sc}^2\, g_s(r)} \sum_{i=1,2,3} \langle \Gamma_{Z_{\mu\tau} \rightarrow N_j N_i} \rangle_{NTH} \left(Y_{Z_{\mu\tau}} - Y_{N_j} Y_{N_i}\right), \end{aligned} \tag{20}$$

Results

DM relic density can be determined from the following relation,

$$\Omega_{DM}h^2 = 2.755\times 10^8\left(\frac{M_{N_2}}{\mathrm{GeV}}\right) Y_{N_2}(T_{\mathrm{Now}}) + 2.755\times 10^8\left(\frac{M_{N_3}}{\mathrm{GeV}}\right) Y_{N_3}(T_{\mathrm{Now}}) \quad . \tag{21}$$

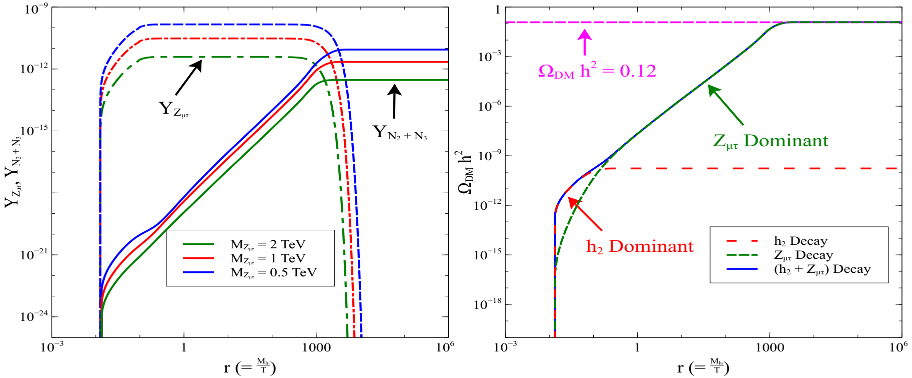

Second Part: FIMP Scalar DM in $U(1)_{B-L}$ model Based on arXiv: 1704.00819 (Accepted in EPJC)

Particles list

Gauge Group	Baryon Fields			Lepton Fields			Scalar Fields		
	$Q_L^i = (u_L^i, d_L^i)^T$	u_R^i	d_R^i	$L_L^i = (\nu_L^i, e_L^i)^T$	e_R^i	N_R^i	ϕ_h	ϕ_H	ϕ_{DM}
$\mathrm{SU(2)_L}$	2	1	1	2	1	1	2	1	1
$\mathrm{U(1)_Y}$	1/6	2/3	−1/3	−1/2	−1	0	1/2	0	0
$\mathrm{U(1)}_{B-L}$	1/3	1/3	1/3	−1	−1	−1	0	2	n_{BL}

Table: Charges of all particles under various symmetry groups.

Type I Seesaw mechanism

$$m_\nu \simeq -\mathcal{M}_\mathcal{D}\,\mathcal{M}_\mathcal{R}^{-1}\mathcal{M}_\mathcal{D}^T\,, \quad (22)$$

$$m_N \simeq \mathcal{M}_\mathcal{R}\,. \quad (23)$$

where $\mathcal{M}_\mathcal{R} = \mathrm{diag}(\mathrm{M_{N_1}}, \mathrm{M_{N_2}}, \mathrm{M_{N_3}})$ and we took $\mathcal{M}_\mathcal{D}$ in the following form,

$$\mathcal{M}_D = \begin{pmatrix} y_{ee} & y_{e\mu} & y_{e\tau} \\ y_{\mu e} + i\,\tilde{y}_{\mu e} & y_{\mu\mu} & y_{\mu\tau} \\ y_{\tau e} + i\,\tilde{y}_{\tau e} & y_{\tau\mu} + i\,\tilde{y}_{\tau\mu} & y_{\tau\tau} \end{pmatrix}, \quad (24)$$

Results

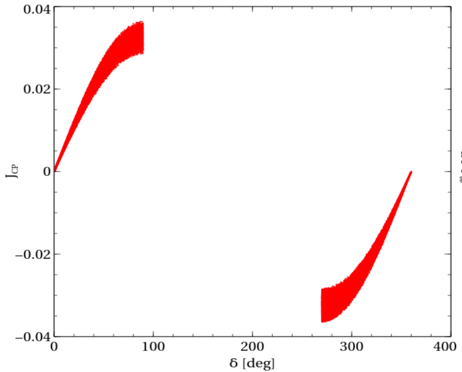
0.04
0.02
0
−0.02
−0.04
J_{CP}
0
100
200
300
400
δ [deg]

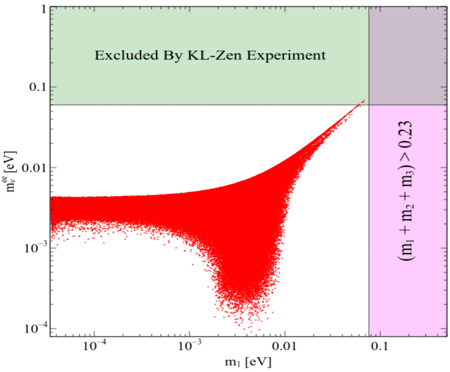
Excluded By KL-Zen Experiment
$(m_1 + m_2 + m_3) > 0.23$
1
0.1
0.01
10^{-3}
10^{-4}
m_ν^{ee} [eV]
10^{-4}
10^{-3}
0.01
0.1
m_1 [eV]

BE for determining Lepton asymmetry[7]

$$
\begin{aligned}
\frac{dY_{N_1}}{dz} &= -\frac{M_{pl}}{1.66\,M_{N_1}^2}\frac{z\sqrt{g_\star(z)}}{g_s(z)}\langle\Gamma_1\rangle\left(Y_{N_1}-Y_{N_1}^{eq}\right)-\frac{2\,\pi^2}{45}\frac{M_{pl}\,M_{N_1}}{1.66}\frac{\sqrt{g_\star(z)}}{z^2}\times \\
&\left(\langle\sigma v\rangle_{N_1,\,Z_{BL}}+\langle\sigma v\rangle_{N_1,t,H_{BL}}\right)\left(Y_{N_1}^2-(Y_{N_1}^{eq})^2\right), \quad (25) \\
\frac{dY_{N_2}}{dz} &= -\frac{M_{pl}}{1.66\,M_{N_1}^2}\frac{z\sqrt{g_\star(z)}}{g_s(z)}\langle\Gamma_2\rangle\left(Y_{N_2}-Y_{N_2}^{eq}\right)-\frac{2\,\pi^2}{45}\frac{M_{pl}\,M_{N_1}}{1.66}\frac{\sqrt{g_\star(z)}}{z^2}\times \\
&\left(\langle\sigma v\rangle_{N_2,\,Z_{BL}}+\langle\sigma v\rangle_{N_2,t,H_{BL}}\right)\left(Y_{N_2}^2-(Y_{N_2}^{eq})^2\right), \quad (26) \\
\frac{dY_{B-L}}{dz} &= -\frac{M_{pl}}{1.66\,M_{N_1}^2}\frac{z\sqrt{g_\star(z)}}{g_s(z)}\left[\sum_{j=1}^{2}\left(\frac{Y_{B-L}}{2}\frac{Y_{N_j^{eq}}}{Y_L^{eq}}+\varepsilon_j\left(Y_{N_j}-Y_{N_j^{eq}}\right)\right)\langle\Gamma_j\rangle\right] \quad (27)
\end{aligned}
$$

[7] Plumacher(1997), Canonical Leptogenesis
N. Okada et al (2010), RL and NM considering two generation of RH neutrinos

$$\varepsilon_2 \simeq -\frac{1}{2}\frac{\mathrm{Im}\left[(\mathcal{M}_{\mathcal{D}}\mathcal{M}_{\mathcal{D}}{}^{\dagger})^2_{12}\right]}{(\mathcal{M}_{\mathcal{D}}\mathcal{M}_{\mathcal{D}}{}^{\dagger})_{11}\,(\mathcal{M}_{\mathcal{D}}\mathcal{M}_{\mathcal{D}}{}^{\dagger})_{22}}\,, \tag{28}$$

$$\varepsilon_1 \simeq -\frac{\Gamma_1\,\Gamma_2}{\Gamma_1^2+\Gamma_2^2}\,\frac{\mathrm{Im}\left[(\mathcal{M}_{\mathcal{D}}\mathcal{M}_{\mathcal{D}}{}^{\dagger})^2_{12}\right]}{(\mathcal{M}_{\mathcal{D}}\mathcal{M}_{\mathcal{D}}{}^{\dagger})_{11}\,(\mathcal{M}_{\mathcal{D}}\mathcal{M}_{\mathcal{D}}{}^{\dagger})_{22}}\,, \tag{29}$$

$$\simeq \frac{2\,\Gamma_1\,\Gamma_2}{\Gamma_1^2+\Gamma_2^2}\,\varepsilon_2\,. \tag{30}$$

Results

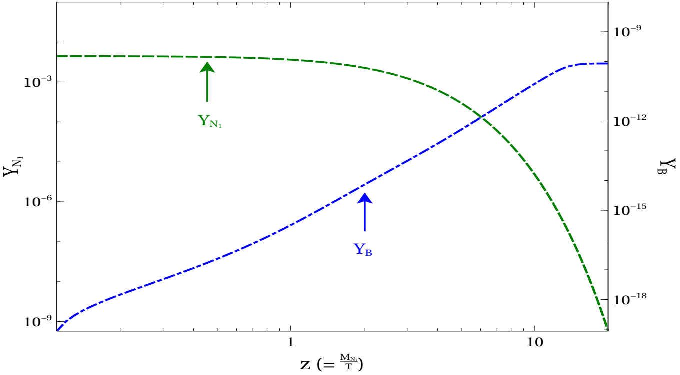

Figure: Baryon asymmetry and RH neutrino decay

BE for calculating DM relic density

$$\frac{dY_{\phi_{DM}}}{dz} = \frac{2M_{pl}}{1.66M_{h_1}^2}\frac{z\sqrt{g_\star(z)}}{g_s(z)}\left[\sum_{X=Z_{BL},\,h_1,\,h_2}\langle\Gamma_{X\to\phi_{DM}\phi_{DM}^\dagger}\rangle(Y_X^{\rm eq}-Y_{\phi_{DM}})\right]$$
$$+\frac{4\pi^2}{45}\frac{M_{pl}M_{h_1}}{1.66}\frac{\sqrt{g_\star(z)}}{z^2}\left[\sum_p\langle\sigma{\rm v}_{p\bar{p}\to\phi_{DM}\phi_{DM}^\dagger}\rangle(Y_p^{{\rm eq}\;2}-Y_{\phi_{DM}}^2)\right.$$
$$\left.+\langle\sigma{\rm v}_{h_1h_2\to\phi_{DM}\phi_{DM}^\dagger}\rangle(Y_{h_1}^{\rm eq}Y_{h_2}^{\rm eq}-Y_{\phi_{DM}}^2)\right], \qquad (31)$$

DM relic density calculated using the following relation,

$$\Omega h^2 = 2.755\times 10^8\left(\frac{M_{DM}}{\rm GeV}\right)\,Y_{\phi_{DM}}(0)\,, \qquad (32)$$

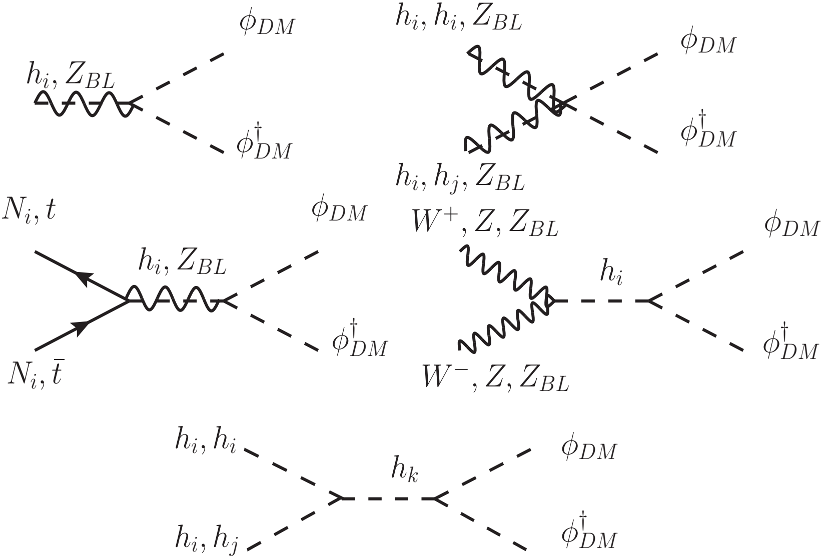

Figure: Relavant Feynman diagrams

Case-I: $M_{DM} < \frac{M_{h_1}}{2}, \frac{M_{h_2}}{2}, \frac{M_{Z_{BL}}}{2}$

SM and BSM particles decay dominated region

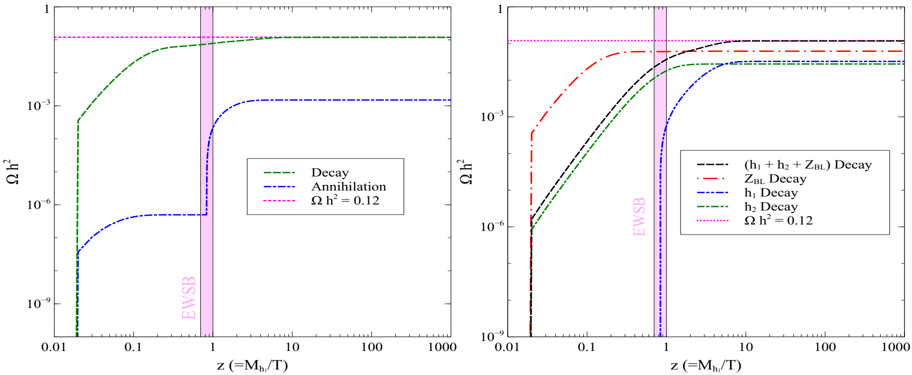

Figure: Parameters value have been kept fixed at $\lambda_{Dh} = 8.75 \times 10^{-13}$, $\lambda_{DH} = 5.88 \times 10^{-14}$, $n_{BL} = 1.33 \times 10^{-10}$, $M_{DM} = 50$ GeV, $M_{Z_{BL}} = 3000$ GeV, $g_{BL} = 0.07$, $M_{h_1} = 125.5$ GeV and $M_{h_2} = 500$ GeV, $\alpha = 10^{-4}$.

Case-II: $\frac{M_{h_1}}{2} < M_{\phi_{DM}} < \frac{M_{h_2}}{2}, \frac{M_{Z_{BL}}}{2}$

BSM particles decay and SM particles annihilation dominated region.

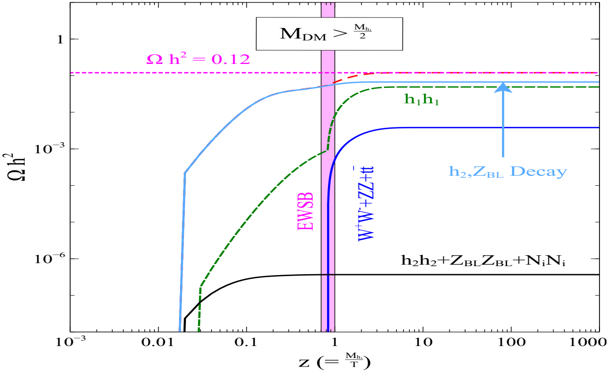

Figure: Parameters value have been kept fixed at $\lambda_{Dh} = 6.364 \times 10^{-12}$, $\lambda_{DH} = 7.637 \times 10^{-14}$, $n_{BL} = 8.80 \times 10^{-11}$, $M_{DM} = 70$ GeV, $M_{Z_{BL}} = 3000$ GeV, $g_{BL} = 0.07$, $M_{h_1} = 125.5$ GeV, $M_{h_2} = 500$ GeV, $\alpha = 10^{-5}$, $M_{N_2} \approx M_{N_1} = 2000$ GeV and $M_{N_3} = 2500$ GeV.

Case-III: $\frac{M_{h_1}}{2}, \frac{M_{h_2}}{2} < M_{\phi_{DM}} < \frac{M_{Z_{BL}}}{2}$

BSM particles decay and annihilation dominated region.

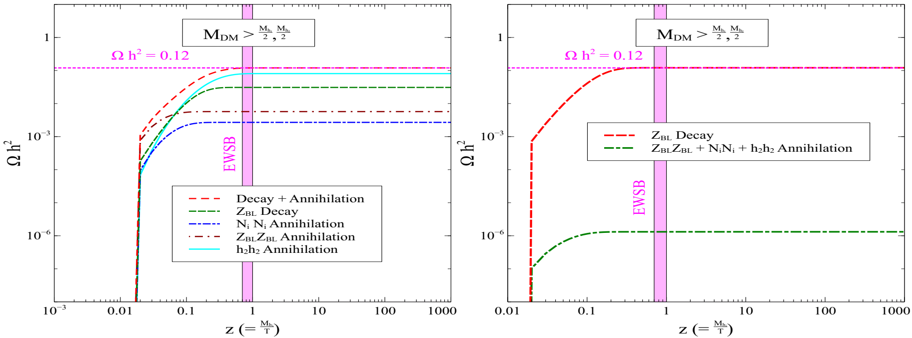

Figure: Parameters value have been kept fixed at $\lambda_{Dh} = 2.574 \times 10^{-12}$ (7.212×10^{-14}), $\lambda_{DH} = 3.035 \times 10^{-11}$ (8.316×10^{-14}), $n_{BL} = 3.4 \times 10^{-11}$ (6.2×10^{-11}), $M_{DM} = 450$ GeV (600 GeV), $M_{Z_{BL}} = 3000$ GeV, $g_{BL} = 0.07$, $M_{h_1} = 125.5$ GeV, $M_{h_2} = 500$ GeV, $\alpha = 10^{-5}$, $M_{N_2} \approx M_{N_1} = 2000$ GeV and $M_{N_3} = 2500$ GeV.

Contd.

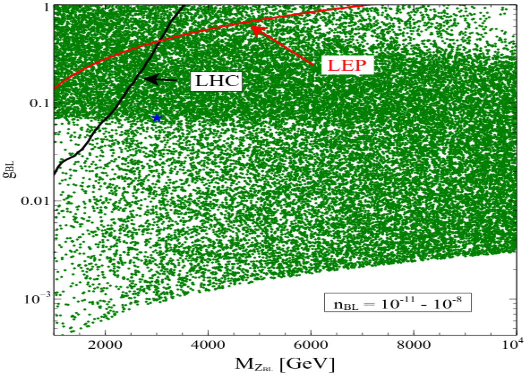

Figure: Green dots satisfy DM relic density in $M_{Z_{BL}} - g_{BL}$. Other relevant parameters used in this plot are $250\,\mathrm{GeV} \leq M_{DM} \leq 5000\,\mathrm{GeV}$, $\lambda_{Dh} = 7.212 \times 10^{-14}$, $\lambda_{DH} = 8.316 \times 10^{-14}$, $M_{h_2} = 500$ GeV, $\alpha = 10^{-5}$, $M_{N_2} \approx M_{N_1} = 2000$ GeV and $M_{N_3} = 2500$ GeV.

Case IV: $M_{\phi_{DM}} > \frac{M_{h_1}}{2}, \frac{M_{h_2}}{2}, \frac{M_{Z_{BL}}}{2}$

BSM particles annihilation dominated region

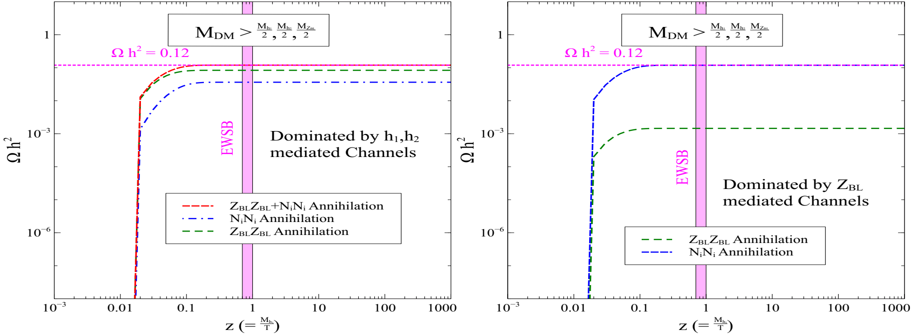

Figure: Relevant parameters value have been kept fixed at $\lambda_{Dh} = 7.017 \times 10^{-12}$ (7.212×10^{-13}), $\lambda_{DH} = 6.307 \times 10^{-11}$ (8.316×10^{-12}), $n_{BL} = 1.0 \times 10^{-10}$ (1.34×10^{-8}), $M_{DM} = 1600$ GeV, $M_{Z_{BL}} = 3000$ GeV, $g_{BL} = 0.07$, $M_{h_1} = 125.5$ GeV, $M_{h_2} = 500$ GeV, $\alpha = 10^{-5}$, $M_{N_2} \approx M_{N_1} = 2000$ GeV and $M_{N_3} = 2500$ GeV.

Contd.

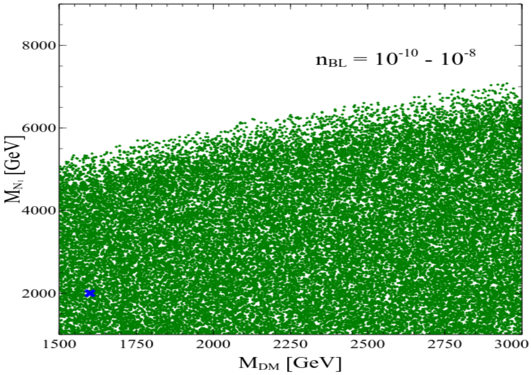

Figure: Allowed region in $M_{DM} - M_{N_1}$ plane which satisfy the observed DM relic density.

Conclusion

- U(1) Models can explain the neutrino mass and oscillation parameters successfully.

Conclusion

- U(1) Models can explain the neutrino mass and oscillation parameters successfully.
- The discrepency in the theoretical and experimental values of muon $(g-2)$ can be addressed within $2\,\sigma$ range.

Conclusion

- U(1) Models can explain the neutrino mass and oscillation parameters successfully.
- The discrepency in the theoretical and experimental values of muon $(g-2)$ can be addressed within $2\,\sigma$ range.
- In the present model we can accomodate both WIMP and FIMP scenario.

Conclusion

- U(1) Models can explain the neutrino mass and oscillation parameters successfully.
- The discrepency in the theoretical and experimental values of muon $(g-2)$ can be addressed within $2\,\sigma$ range.
- In the present model we can accomodate both WIMP and FIMP scenario.
- GC γ-ray excess (observed by Fermi-LAT) can be explained by WIMP DM candidate.

Conclusion

- U(1) Models can explain the neutrino mass and oscillation parameters successfully.
- The discrepency in the theoretical and experimental values of muon $(g-2)$ can be addressed within $2\,\sigma$ range.
- In the present model we can accomodate both WIMP and FIMP scenario.
- GC γ-ray excess (observed by Fermi-LAT) can be explained by WIMP DM candidate.
- In $U(1)_{B-L}$ model, we have combinely studied neutrino mass, leptogenesis and DM.


Thank you